

Article

Application of HEC-HMS in a Cold Region Watershed and Use of RADARSAT-2 Soil Moisture in Initializing the Model

Hassan A. K. M. Bhuiyan ^{1,*}, Heather McNairn ², Jarrett Powers ¹ and Amine Merzouki ²

¹ Science and Technology Branch, Agriculture and Agri-Food Canada, Winnipeg, MB R3C 3G7, Canada; Jarrett.Powers@AGR.GC.CA

² Science and Technology Branch, Agriculture and Agri-Food Canada, Ottawa, ON K1A 0C6, Canada; Heather.McNairn@AGR.GC.CA (H.M.); Amine.Merzouki@AGR.GC.CA (A.M.)

* Correspondence: akmh.bhuiyan@gmail.com; Tel.: +1-204-771-9666

Academic Editor: Luca Brocca

Received: 15 November 2016; Accepted: 2 February 2017; Published: 9 February 2017

Abstract: This paper presents an assessment of the applicability of using RADARSAT-2-derived soil moisture data in the Hydrologic Modelling System developed by the Hydrologic Engineering Center (HEC-HMS) for flood forecasting with a case study in the Sturgeon Creek watershed in Manitoba, Canada. Spring flooding in Manitoba is generally influenced by both winter precipitation and soil moisture conditions in the fall of the previous year. As a result, the soil moisture accounting (SMA) and the temperature index algorithms are employed in the simulation. Results from event and continuous simulations of HEC-HMS show that the model is suitable for flood forecasting in Manitoba. Soil moisture data from the Manitoba Agriculture field survey and RADARSAT-2 satellite were used to set the initial soil moisture for the event simulations. The results confirm the benefit of using satellite data in capturing peak flows in a snowmelt event. A sensitivity analysis of SMA parameters, such as soil storage, maximum infiltration, soil percolation, maximum canopy storage and tension storage, was performed and ranked to determine which parameters have a significant impact on the performance of the model. The results show that the soil moisture storage was the most sensitive parameter. The sensitivity analysis of initial soil moisture in a snowmelt event shows that cumulative flow and peak flow are highly influenced by the initial soil moisture setting of the model. Therefore, there is a potential to utilize RADARSAT-2-derived soil moisture for hydrological modelling in other snow-dominated Manitoba watersheds.

Keywords: RADARSAT-2; flood forecasting; soil moisture accounting (SMA); HEC-HMS

1. Introduction

Flooding is a common occurrence in the Red and Assiniboine River sub-basins; part of the larger Lake Winnipeg basin in Southern Manitoba, Canada. Of the ten highest recorded floods on the Red River dating back to the 1800s, four have occurred in the last twenty years. This includes the 1997 flood, which stands as the third largest flood ever recorded on the Red River. In 2011, the Assiniboine River experienced a one in 145 year flood and the largest in recorded history lasting over 120 days [1]. Floods of this magnitude have a devastating impact, resulting in damage to homes, infrastructure and lost agricultural production. Costs for recovery programs and investments in flood infrastructure are shared by all levels of government and cost billions of dollars [2].

The majority of Manitoba floods are caused by spring snowmelt (freshet) events in late April and May [3]. Spring flooding in Manitoba watersheds is greatly influenced by the soil moisture condition of the previous fall along with the snow received in the watershed [2,4]. The freeze-thaw cycle in

Manitoba is connected to flooding and the timing of the peak. The ground often stays frozen while the surface snow begins to melt. This can create dramatically large volumes of surface runoff, as there is low to null soil infiltration. The freeze-thaw cycle can act as the trigger of flooding [5]. These physical processes need to be considered in order to provide accurate flood forecasting.

Watershed models are tools to incorporate all relevant surface processes to provide runoff volumes for flood forecasting. Presently, the Hydrologic Forecast Center (HFC) of Manitoba is using the Manitoba Antecedent Precipitation Index (MANAPI) model for flood forecasting in Manitoba. MANAPI is an event-based model, computing a single runoff value for a watershed or sub-watershed from rain or snowmelt events. The model computes snowmelt from historical events representing either average, rapid or gradual melt. MANAPI uses a relationship that relates runoff to the ‘total winter precipitation’ and the ‘antecedent precipitation index (API)’. The relationship is based on historical events and is unique to the watershed. Therefore, it cannot simulate a unique runoff response that has not been experienced in the past and which is significantly different from the average of the historical events. MANAPI is not capable of computing runoff from events that involve a significant variation in input, such as freeze-melt cycles. There are other known limitations of MANAPI in addressing complex watershed processes, such as precipitation and depression storage [6]. The MANAPI was last reviewed in 1985. Since then, many developments in hydrologic modelling procedures have occurred. The 2013 Flood Task Force recommended that the Province of Manitoba should examine other hydrological models to assess which model may best meet its forecasting requirements [2]. As a result of the recommendation, the HFC has selected the Hydrologic Modelling System developed by the Hydrologic Engineering Center (HEC-HMS) as one of the models to be tested. HEC-HMS was selected due to its flexibility and applicability in other regions for flood forecasting.

The uncertainty in flood forecasting is largely associated with hydro-meteorological input and the selection of hydrological model parameters [7,8]. There are known sources of uncertainty in initialization of the model for soil moisture. Soil moisture estimates from satellite data are increasingly used for hydrological modelling, as measured data are sparse [9,10]. Tramblay et al. [11] stated that satellite data products are able to reproduce reasonably accurate daily soil moisture dynamics at the catchment scale. Li et al. [12] presented recent advancements on integrating remotely-sensed satellite soil moisture data using a rainfall-runoff model for rain fall-driven flood forecasting. Massari et al. [13] used the initial wetness condition from globally available soil moisture retrievals in a simplified rainfall-runoff model to simulate rainfall events in a Mediterranean catchment. Xu et al. [14] provided a review on the integration of remote sensing data and hydrological modelling. Soil moisture measurements derived from satellite data were reported to be an improvement over field measured data due to improved spatial scale. Furthermore, several studies confirmed the use of satellite estimates of antecedent wetness conditions for flood modelling [9,11]. Knowing the importance of antecedent soil moisture in flood event modelling, none of these studies attempted integrating remotely-sensed soil wetness to provide the initial setting of a cold region’s hydrological model. McNairn et al. [15] tested the accuracy of RADARSAT-2 data to estimate surface soil moisture and were able to estimate volumetric soil moisture with a root mean square error (RMSE) of 5.37%. Given these advancements, this study will examine the applicability of using soil moisture data derived from the RADARSAT-2 satellite as initial setting values of HEC-HMS in simulating flood events in a cold region watershed. The specific objectives of the current research are as follows:

- (a) to assess the usability/applicability and potential benefits of HEC-HMS using RADARSAT-2-derived soil moisture estimates in the snowmelt-dominated Sturgeon Creek watershed and;
- (b) to test the sensitivity of initial soil moisture in setting the HEC-HMS model for flood forecasting.

2. Study Area and Data

The Sturgeon Creek watershed is located northwest of the City of Winnipeg, Manitoba, Canada. Figure 1 illustrates the geographic location of the watershed along with the location of a flow gauge (ID#05MJ004) and three weather stations. The watershed has an effective drainage area of 545 km². The watershed slopes towards the southeast and flows through the Rural Municipality of Rosser and through the City of Winnipeg before discharging into the Assiniboine River. The landscape is relatively flat with elevations ranging from a high of 279 m (upstream) and 231 m. The upper reaches of the watershed are higher sloped (up to 1.2%) compared to the middle and lower reaches (as low as 0.05%). Soils in the upstream portion of the watershed are composed of a thin layer of black to dark grey clay loams overlying a mixed parent material of lacustrine clay and extremely calcareous clay loam tills. The middle reach of the watershed is a nearly level landscape with stratified layers of loam, fine sand and deep lacustrine clay deposits. The lower reach is a level landscape with thick lacustrine clay deposits. As such, surface drainage is very slow, resulting in the development of surface drains and stream channelization to improve the flow of water off agricultural lands. Agriculture is the dominant land use in the watershed with 75% of the land base devoted to annual crop production. Forage and pasture grasslands account for 16% of the land cover. Wetlands are less than 1% [16,17]. LiDAR (light detection and ranging) elevation data, provided by the Province of Manitoba, are used for GIS analysis to derive topographic information for HEC-HMS modelling and to delineate the watershed. Different watershed data, such as precipitation, snow depth and outflow, were collected and examined to identify dominant hydrological processes.

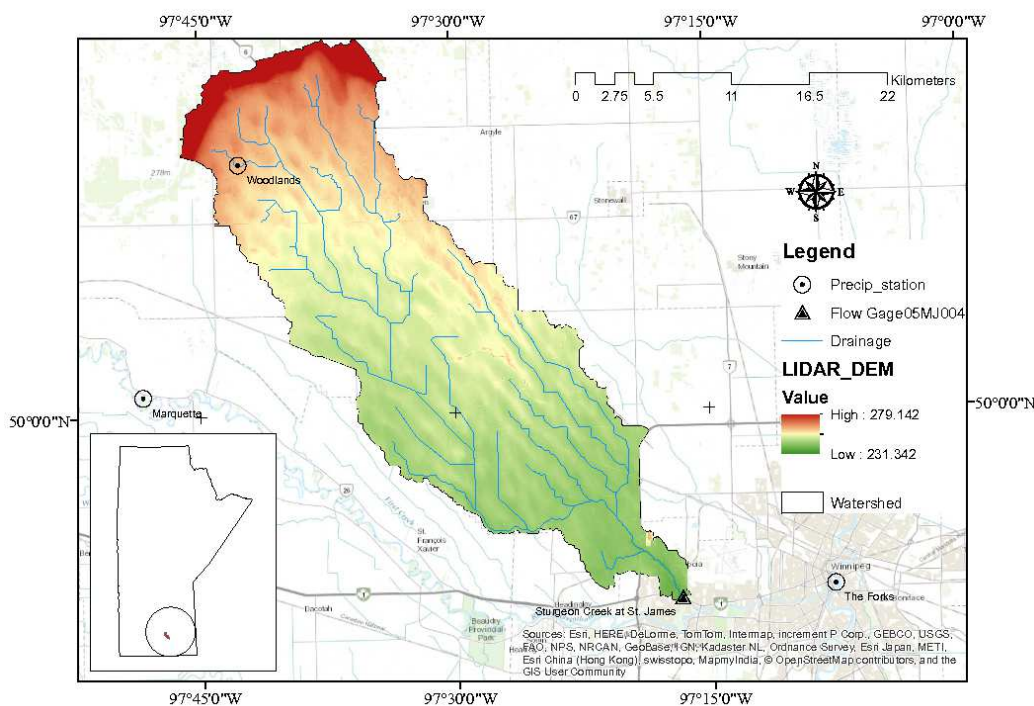


Figure 1. Study area: Sturgeon Creek watershed in Manitoba, Canada. The index map shows the provincial boundary and the location of the watershed in the circle.

2.1. Flow Data

Discharge data used in this study were collected from the Water Survey Canada (WSC) data portal. The Water office provides public access to real-time hydrometric data through the <https://wateroffice.ec.gc.ca/> site, accessed on 4 July 2015 at the Sturgeon Creek (#05MJ004) gauging station located at St. James. The geographic location of the station is at latitude 49°52' 54" N and longitude

97° 16' 47" W. The gauge station measures seasonal flow data from 1 March–31 October. Annual peak flows (1965–2014) from the Sturgeon Creek gauge were analysed. During this time, the highest daily flow of $82.7 \text{ m}^3/\text{s}$ was recorded in 1974. Two other high peak flows of $67.1 \text{ m}^3/\text{s}$ and $63.2 \text{ m}^3/\text{s}$ were recorded in 2009 and 1979, respectively. The time series of peak flows were segmented into five ten-year intervals in order to evaluate dry-wet hydrological cycles. Jacob and Lorenz [18] used ten-year segments to examine variability and trends of a hydrologic cycle. Figure 2 depicts the five ten-year intervals of daily average flow at the gauge station and shows that the peak of the creek appears during the spring snowmelt.

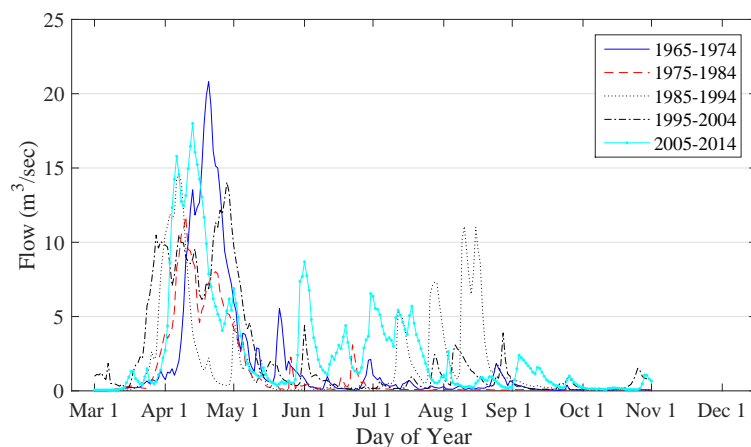


Figure 2. Flow data (1965–2014): average of ten-year segments at the Sturgeon Creek (#05MJ004) gauging station.

2.2. Weather Data

Precipitation and temperature data used in this study were obtained from two Environment Canada and Climate Change (ECC) weather stations at Winnipeg and Marquette, as well as one Manitoba Agriculture (MA) weather station at Woodlands. The locations of the weather stations are shown in Figure 1. The daily meteorological data used in the modelling were reviewed for consistency, and any missing records were replaced with data from nearest neighbouring stations. Sub-watershed temperatures were assigned from the closest neighbouring station, and a lapse rate of $5 \text{ }^\circ\text{C}/1000 \text{ m}$ was used. Precipitation data were interpolated across the sub-watershed using the inverse-distance-squared weighting method.

The weather station at Marquette is selected as the representative station due to data availability and quality. The climate normal (1971–2000) of the station shows the average high and low temperature as $19.5 \text{ }^\circ\text{C}$ and $-17.5 \text{ }^\circ\text{C}$ for the months of July and January, respectively. The mean annual average temperature is $2.9 \text{ }^\circ\text{C}$. Precipitation statistics at the Marquette station shows that the watershed receives most summer rainfall starting from the middle of May to the end of July. Average annual precipitation (2005–2014) recorded at the Marquette station is 540 mm, whereas the highest and lowest annual precipitation received at the station is 790 mm and 328 mm, respectively.

Figure 3 provides a plot of snow depth over 10 years at the Marquette station. Depending on the snow year, maximum depth varies from 20 cm–60 cm. At the Marquette station, snow starts to accumulate in the middle of November. Snow melt typically begins the first week of March and is finished by the end of April. The snowmelt may act as the trigger of flooding [5]; therefore, evaluating the snow depth variable may provide more insight into the interaction of hydrological processes within the watershed.

Although during event modelling, water loss due to evaporation may be neglected, it must be included for continuous modelling. The monthly evaporation values were estimated for the entire watershed using Thornwaite's method [19]. Calculated monthly evapo-transpiration (ET) values were entered manually for each sub-watershed with a coefficient value of 0.7. The model calculates

the potential ET as the product of the monthly value and the coefficient for all time periods of the month according to the model's setting [20]. Thornwaite's methodology is adopted to estimate ET, as only temperature data were available.

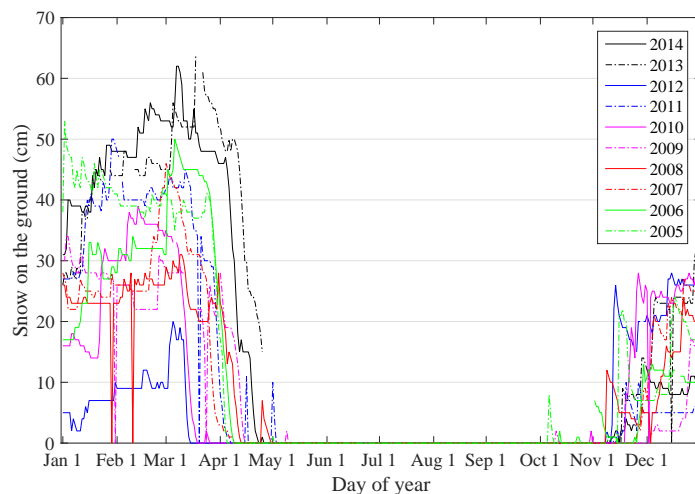


Figure 3. Snow depth (in cm) measured at the Marquette station.

2.3. Soil Moisture Estimates from RADARSAT-2 Satellite Data

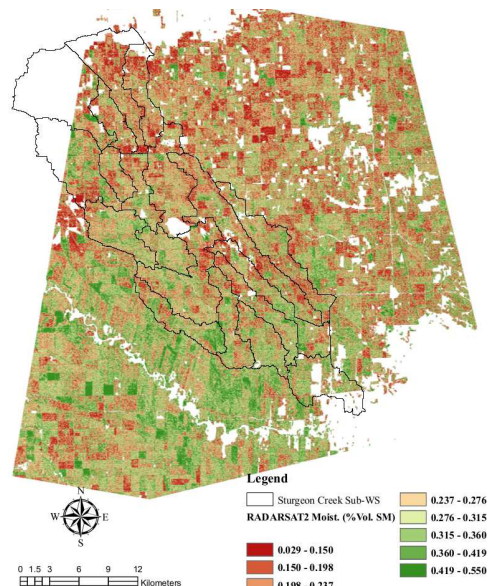
RADARSAT-2 is a synthetic aperture radar (SAR) satellite operating at 5.4 GHz. The intensity of microwave energy scattered at this frequency is primarily driven by the dielectric constant (and hence, the amount of water) in a target illuminated by the satellite. The physically-based integral equation model (IEM) is used to estimate the volume of moisture in the top few centimetres of the soil, using backscatter intensity recorded by RADARSAT-2 [21,22]. The real dielectric constant is retrieved using backscatter at horizontal transmit-horizontal receive (HH) and vertical transmit-vertical receive (VV) polarizations and the local SAR incident angle. Volumetric soil moisture is then derived from the real dielectric constant using a dielectric mixing model. RADARSAT-2 was programmed to acquire an image over the Sturgeon Creek Watershed, on 15 October 2014 (Figure 4a). This was the last satellite acquisition date available prior to the soil freeze-up. As the soil temperature approaches zero, the dielectric properties of the water in the soil change. Under frozen conditions, backscatter is no longer sensitive to the soil dielectric, and thus, inversion of RADARSAT-2 data for soil moisture is not valid. Data were collected by the three Real-time In-situ Soil Monitoring for Agriculture (RISMA) stations. RISMA stations data operated by Agriculture and Agri-Food Canada (AAFC) can be obtained through the <http://aafc.fieldvision.ca/> site, accessed on 14 November 2016. The stations located in the watershed confirmed that for all RADARSAT-2 acquisition after 15 October 2014, soil temperature was below freezing. The 15 October acquisition was the closest available image before the freeze-up and, thus, was used to establish the initial soil moisture state given that the soil moisture remains static once soils have frozen. The output image is a pixel-by-pixel estimate of percent volumetric soil moisture, θ ($m^3 m^{-3}$), at a spatial resolution of 13.6 m. Pixel-based estimates of soil moisture were then binned into eight moisture intervals. In Figure 4a, pixels displayed in red shades represent soils at lower saturation, and green-toned pixels represent higher saturation. White areas are regions outside of the satellite image or non-annual cropped areas (grasslands, trees, urban, open water) where soil moisture values cannot be retrieved. The estimated soil moisture ranges between $0.029\ m^3 m^{-3}$ and $0.550\ m^3 m^{-3}$ over the area. ArcGIS was used to overlay the pixel-based (rasterized) soil moisture product with the sub-watershed polygons to calculate average soil moisture values for each sub-watershed (Figure 4b) excluding no data pixels. The image did not cover the entire watershed (i.e., the missing part of Sub-watersheds W670 and W780). Average soil moisture

for Sub-watersheds W670 and W780 were estimated assuming similar soil moisture retrievals for the missing part of the sub-watershed. The HEC-HMS model requires soil saturation (in percent), which is calculated using Equation (1).

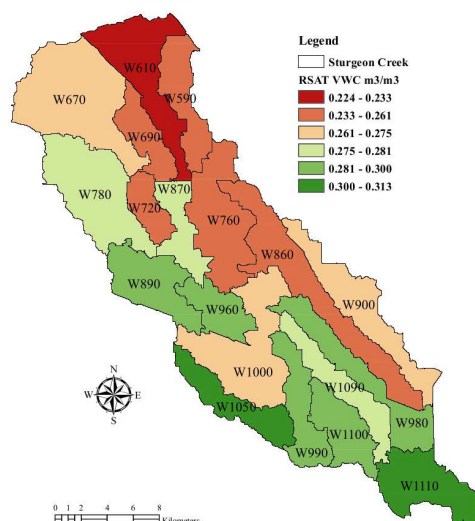
$$S = \theta \times \phi^{-1} \times 100 \quad (1)$$

$$\phi = 1 - \rho_b / \rho_s \quad (2)$$

where S is the saturation percentage, θ is the volumetric water content from RADARSAT-2 data, ϕ is porosity, ρ_b is bulk density and ρ_s is specific density. Three measured bulk densities of 1.04, 1.39 and 1.32 gm/cm^3 are used in this study for the southern, middle and northern sub-watersheds of Sturgeon Creek, respectively [23]. Soil porosity (ϕ) is calculated following Equation (2) using specific density (ρ_s) as 2.65 gm/cm^3 .



(a) Soil moisture binned into eight intervals.



(b) Pixel-based soil moisture ($\text{m}^3 \text{m}^{-3}$) averaged over the sub-watershed.

Figure 4. Soil Moisture retrieved using a RADARSAT-2 satellite image acquired on 15 October 2014.

2.4. Fall Soil Moisture Survey Data

Each year, Manitoba Agriculture prepares a fall soil moisture map using field survey data. Details of fall soil moisture maps can be seen from <http://www.gov.mb.ca/agriculture/environment/soil-management/manitoba-fall-soil-moisture-survey.html>. These maps are generated from core samples that are taken from approximately 100 fields across southern Manitoba. The fields are sampled in mid-late October, prior to freeze-up. The samples are weighed and oven-dried to determine their soil moisture level. The 2014 surface (0–30 cm) soil moisture map is used to establish the initial state of soil moisture for the event modelling. Due to the sparse measurements and highly generalized nature of the fall soil moisture survey, one soil moisture value of 40% is used to represent the initial saturation for the entire watershed.

3. HEC-HMS Model

The HEC-HMS model is designed to simulate the complete hydrological processes of a dendritic watershed system [24]. The model can be applied to analyse flooding, flood frequency, flood warning system planning, reservoir and spillway capacity studies, etc. [25]. The model can be used for both continuous and event-based modelling. Many researchers have successfully used HEC-HMS [26–28] for flood event modelling. The soil moisture accounting (SMA) algorithm has been successfully used in continuous simulation of the model [29–31]. A snow model is essential in order to capture flood peak and timing in the spring snow melt-dominated watersheds in Manitoba [2]. Gyawali and Watkins [32] tested the temperature index snow accumulation and melt algorithm of HEC-HMS in snow-affected watersheds in the Great Lakes basin. However, no studies have reported the application of HEC-HMS in a snow-dominated Manitoba, Canada, watershed.

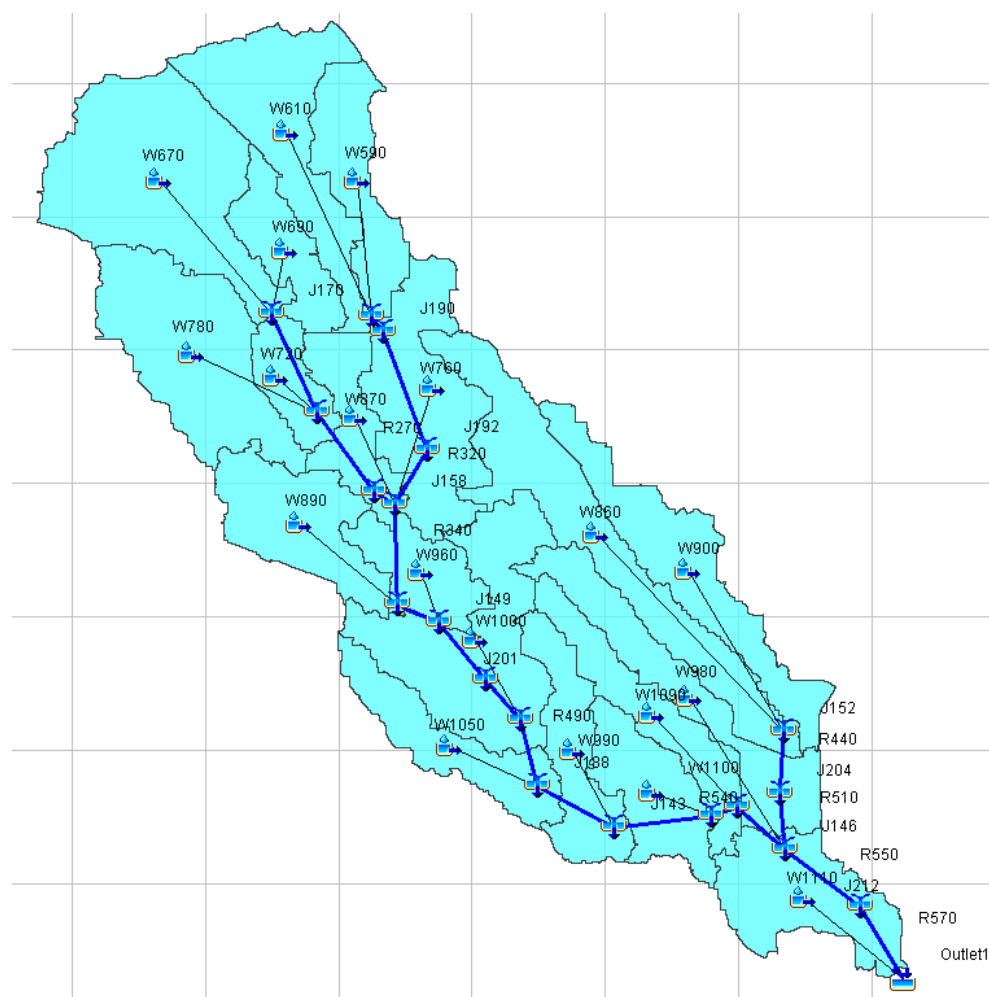
The HEC-HMS (Version 4.0) model is grouped into four major input components, such as the watershed model, the meteorological model, the data manager and the control manager. The watershed model is the representation of real-world objects and describes the different elements of the hydrological system, such as sub-watershed, reaches, junctions, sources, sinks, reservoirs and diversions. Each of these elements needs some parameters to define their interaction in a hydrological system. These elements are inter-linked to facilitate the flow of water and to create a dendritic network [24]. Table 1 provides a list of different parameter methods selected in the watershed model. A simple canopy is selected, as no changes of canopy (i.e., dynamic canopy) are expected. A simple surface is selected to provide simple representation of the soil surface where rainfall on the soil surface is stored until the storage capacity of the surface is filled.

In order to set-up the HEC-HMS for the Sturgeon Creek Watershed, a hydrologically-corrected DEM was created from LiDAR data by re-sampling the DEM at a 15-m resolution. River network, road network and bridge/culvert data from the Manitoba Land Initiative (MLI) were used to create a hydrologically-conditioned DEM. Land cover and soil properties were also processed and re-classed using ArcGIS. Terrain pre-processing steps, such as filling sink, flow direction, flow accumulation, stream/drainage line processing and watershed delineation, were performed using ArcHydro Tools and ArcGIS. The HEC-GeoHMS was used to extract physical parameters necessary for the HEC-HMS model setup. The HEC-HMS can easily import the setup data from HEC-GeoHMS to construct a project and schematic for the model.

Figure 5 presents a schematic of the Sturgeon Creek Watershed prepared by HEC-HMS. The schematic shows sub-watersheds, reaches, junctions, sources and sinks of the watershed. The HEC-HMS was set up as a semi-distributed model by sub-dividing the catchment into 19 sub-watersheds. The sub-division of the catchment is performed by following the stream and road network, as well as underlying soil properties. The semi-distributed setup allowed us to examine governing hydrological processes in the sub-watersheds.

Table 1. Selected methods of HEC-HMS model.

Basin Model		Meteorological Model	
Parameter Method	Selected Method	Parameter Method	Selected Method
Canopy	Simple Canopy	Precipitation	Inverse Distance
Surface	Simple Surface	Evaporation	Monthly Average
Transform	SCS Unit Hydrograph	Snowmelt	Temperature Index
Base Flow	Recession	Shortwave	None
Routing	Muskingum		
Loss	Soil Moisture Accounting		

**Figure 5.** The schematic of the Sturgeon Creek Watershed created by HEC-HMS. The naming of sub-watersheds, reaches and junctions begins with W, R and J, respectively.

The HEC-HMS tracks snowmelt and accumulation using the temperature index method. Melt rates are calculated dynamically based on the current atmospheric condition and past conditions of the snow pack. The temperature index method was set up and calibrated in order to capture the spring snow melt peak. This method is governed by a threshold temperature, which separates snowfall from rainfall denoted by $PX_{\text{temperature}}$. There is a base temperature that distinguishes melt from non-melt periods of snow. The temperature index method does not account for sublimation from and condensation to the snow pack. The final calibrated parameter values are shown in Table 2. The antecedent temperature index (ATI) melt-rate and cold-rate functions are specified separately

in the model. The temperature index model includes parameter data for each sub-watershed in the meteorological model. Each sub-watershed must have one elevation band defined in the meteorological model.

In this study, the SMA method was used to account for vegetative canopy retention and to simulate the movement of water through the soil surface and the deeper soil profile to the groundwater layers [20]. These layers provide wetting and recovery cycles of soil moisture for long-term continuous hydrological simulations. SMA requires the initial soil moisture condition to be specified at the beginning of the simulation. The soil moisture map derived from RADARSAT-2 (Figure 4) was used as the basis of initial soil moisture. The HEC-GeoHMS was used to build a project setup for the SMA loss method. The parameters needed for SMA (maximum infiltration rate, soil storage, tension zone storage and soil zone percolation rate) were estimated using Manitoba land use, land cover and soil databases. Soil profile data were also used for the estimation of soil parameters of the SMA model. The soil percolation rate was based on the average hydraulic conductivity of soil profile data. The SCS unit hydrograph was used with lag time estimated by employing HEC-GeoHMS with an empirical relationship. The recession method is used for base flow calculation. The simple Muskingum routing is selected to route flow through the channel.

Table 2. Snow melt input parameters for the temperature index method.

Parameter	Unit	Value
PX Temperature ^a	°C	1.7847
Base Temperature	°C	0.6294
Wet Melt Rate	mm/°C-day	0.9876
Rain Rate Limit	mm/day	2
ATI ^b -Melt Rate Coefficient	-	0.9995
Cold Limit	mm/day	20
ATI-Cold Rate Coefficient	-	0.9995
Water Capacity	%	10
Ground Melt	mm/day	0

^a The PXtemperature is used to differentiate between precipitation falling as rain or snow; ^b Antecedent Temperature Index.

3.1. Model Evaluation

Model calibration and validation were conducted based on simulated and observed daily flow data at the gauging station. The model parameters were first calibrated using automated calibration methods available in the HEC-HMS model. The automated calibration procedure uses an iterative method to minimize the objective function in order to obtain agreement between simulated and observed flow data [24]. The precise adjustments of parameters were obtained through manual calibration.

Many different test criteria have been developed to assess the efficiency of a hydrological model calibration [33–35]. For this study, the Nash–Sutcliffe (N_s) coefficient of model efficiency [36] and the deviation of runoff volumes (D_v) were used to measure the goodness-of-fit between the observed and simulated flow time series. Higher values of N_s (closer to one) indicate better agreement. Henriksen et al. [37], Table 4, suggested that values of N_s between 0.5 and 0.65 are good; 0.65–0.85 are very good; and >0.85 are excellent. For a perfect model the D_v is equal to zero. The D_v value emphasizes volume conservation and is not sensitive to errors in streamflow timing or seasonality.

A sensitivity analysis of the model was performed to understand the complex relationships amongst model parameters and variables. The sensitivity analysis determines which parameters significantly impact model performance and provides an estimate of the precise value of each parameter. This analysis of SMA parameters was conducted by varying each input parameter by ±10% on each step without changing other parameters.

4. Results and Discussion

The HEC-HMS model simulations were performed for a single flood event, as well as continuous simulation over the Sturgeon Creek Watershed.

4.1. Event Modelling

The HEC-HMS event model was set up for a 28 March 2015 (12:00) to 6 April 2015 (12:00) flood event. The event hydrological modelling was performed using hourly time steps to understand fine-scale hydrological processes and to respond to the quantity of surface runoff, peak and timing of peak. Two event simulations are presented in this study to demonstrate the benefits of using the initial state of soil moisture measurement from satellite data. Simulation 1 utilizes one soil moisture value from the Fall Soil Moisture Survey. Simulation 2 is performed using soil moisture values for each sub-watershed estimated from RADARSAT-2. Results from the event simulation are presented in Figure 6.

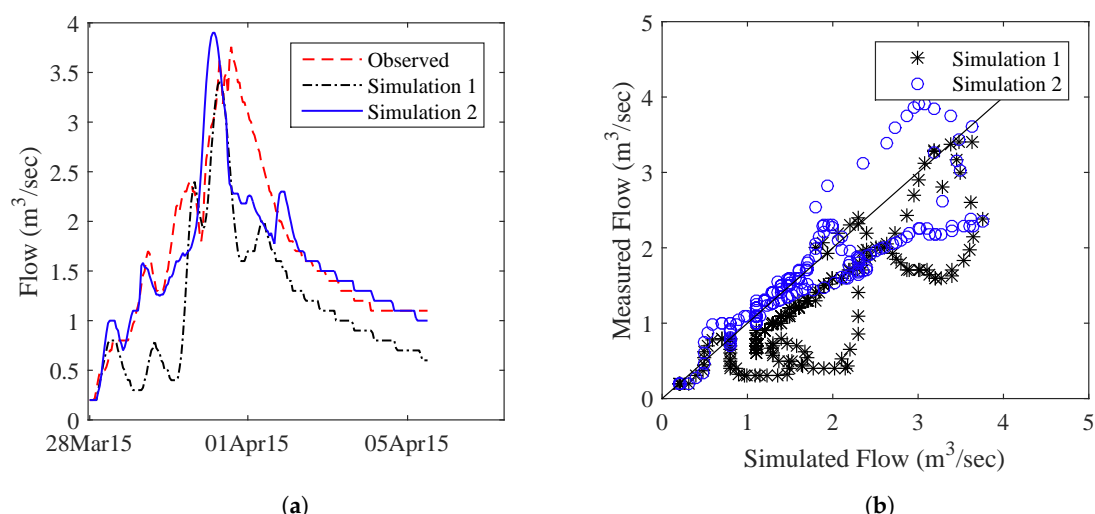


Figure 6. Event modelling of hourly flow series on an event of 28 March 2015 (12:00) to 6 April 2015 (12:00) for the Sturgeon Creek Watershed. Simulation 1 utilizes one soil moisture value from the Fall Soil Moisture Survey, while Simulation 2 utilizes initial soil moisture values from RADARSAT-2. (a) Comparison of the observed and simulated hydrograph; (b) the distribution of points is shown from the $y = x$ line.

The comparison of observed and simulated hourly flow series of the event using RADARSAT-2 shows that the simulated peak matches well (within 3%) with the peak values of measured flow. However, the timing of the simulated peak was earlier than that observed. Furthermore, the small peaks of the simulated flow series did not match with the observed. These small peaks may be the result of localized melt events, which could not be captured by the model. The Nash–Sutcliffe coefficient of efficiency (N_s) and the deviation of runoff volume (D_v) are found to be 0.74 and -4.83% , respectively. These values are within acceptable ranges.

The simulated hourly flow series of the event using data from the Fall Soil Moisture Survey does not agree well with the observed flow event. The event peak was underestimated by -10% ; and other small peaks were also underestimated. The model performance measures N_s and D_v were 0.31 and -34.2% , respectively. The two simulations differ only in the state of initial soil moisture. The difference in the generation of peaks in the event model simulations was clear. Given the small number of sampling points and the generalization of the data of the Fall Soil Moisture Survey, only one surface soil moisture value can be used to represent the initial saturation value of the watershed.

With the differences in soil, landscapes and precipitation, this value may not be representative of soil moisture within the individual sub-watersheds. The initial melt at the surface may have been retained at the sub-watershed and added to the soil water content to reach a threshold before contributing to runoff at the outlet. This could be the most probable reason of underestimating the peak flow and cumulative outflow. A sensitivity test of initial soil moisture is provided in Section 4.3.2.

4.2. Continuous Modelling

The parameters obtained from the calibrated HEC-HMS for event modelling were used to set up a continuous simulation. The continuous simulation was performed with the SMA model using a daily time step and compared with flow series of 1 March 2014–1 June 2014. A continuous multi-year simulation was not done in this watershed, as measured flow data are only available from 1 March–31 October each year.

Figure 7a presents a comparison of observed and simulated output from the continuous modelling of daily flow series for the Sturgeon Creek Watershed. The model simulated timing of the peak matches well, but the peak flow is overestimated by 21%. Furthermore, other small peaks were not well captured. The deviation of runoff volume (D_v) was -17.9% ; the Nash–Sutcliffe coefficient of efficiency (N_s) was 0.87. Figure 7b presents the scatter plot of simulated flow vs. measured flow and shows a strong positive correlation (0.95). The line of correlation 1.0 (i.e., $y = x$ line) is also shown in the plot.

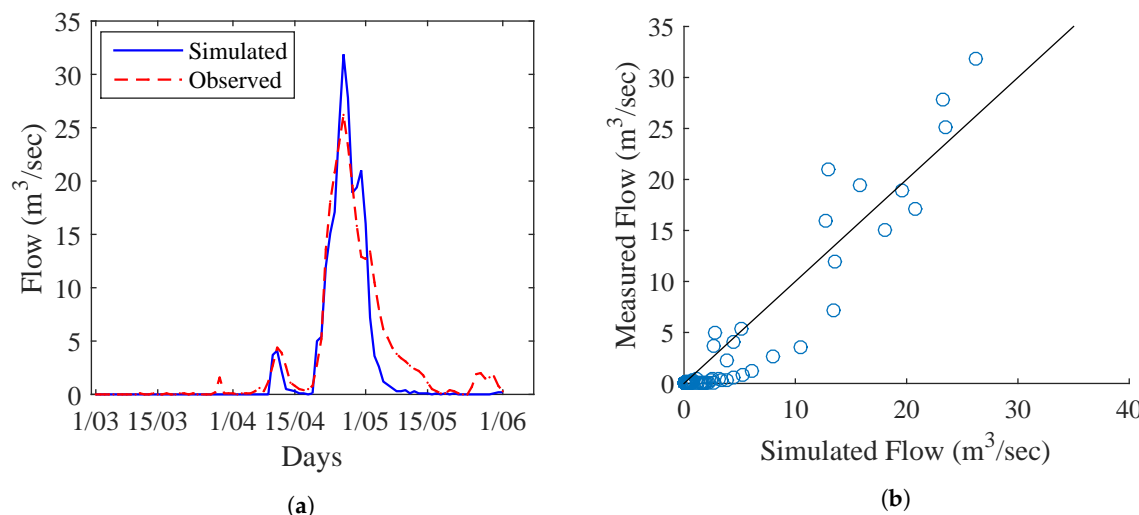


Figure 7. Continuous modelling of daily flow series for the Sturgeon Creek Watershed. The calibration is performed for 2014 from 1 March 2014–1 June 2014. (a) Comparison of observed and simulated hydrograph; (b) distributions of points are shown from the $y = x$ line.

A second continuous model simulation was performed for 2011 using the 2014 parameters. Figure 8a depicts simulated flow data compared to observed flows. The 2011 simulation also shows that the timing of peak flow arrival is well captured, but the peak flow volume is over-estimated by 13%. The D_v and N_s were found to be -7.22% and 0.88, respectively. Figure 8b presents the scatter plot, which shows a strong positive correlation (0.94).

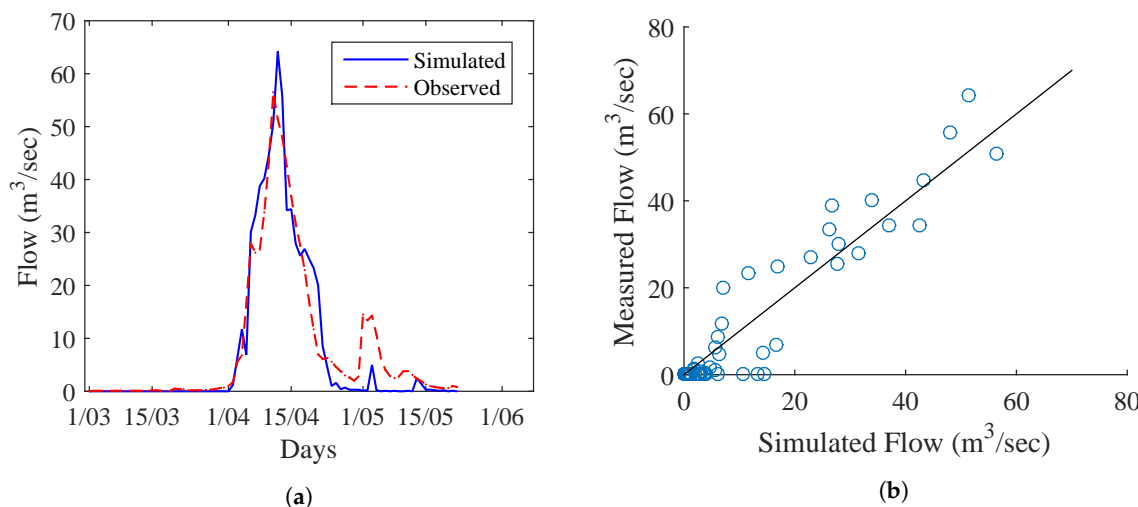


Figure 8. Continuous modelling of daily flow series for the Sturgeon Creek Watershed. The validation is performed for 2011 starting from 1 March 2011–1 June 2011. (a) Comparison of observed and simulated hydrograph; (b) distributions of points are shown from the $y = x$ line.

The model performance results are summarized in Table 3. Event Simulation 2 showed improved performance over Simulation 1 due to well-defined initial soil moisture values from the RADARSAT-2 satellite data in all sub-basins. Performance indicators presented in Table 3 also reveal that the flow simulations generated by the HEC-HMS model are suitable for the Sturgeon Creek Watershed. Several authors [33,38,39] have successfully used these indicators for the performance evaluation of hydrological models. Henriksen et al. [37], Table 4, suggest that values of N_s obtained in this study are in very good agreement.

Table 3. Performance measures of the HEC-HMS model.

Model Simulation	Duration	Dev. of Runoff Volume, D_v (%)	Nash Co-efficient, N_s
Event (Simulation 2)	28 March 2015–6 April 2015	−4.83	0.74
Event (Simulation 1)	28 March 2015–6 April 2015	−34.25	0.31
Continuous	01 March 14–1 June 2014	−17.9	0.87
Continuous	01 March 11–1 June 2011	−7.22	0.88

The snow melt process is important for this Manitoba watershed due to spring flooding [3]. The snow depth data from the ECC station at Marquette were used for validation in this study. Following the method described by Strum et al. [40], the snow depth was converted to snow water equivalent (SWE) using a bulk density value of 0.312 gm/cm^3 . The HEC-HMS simulates SWE as an internal variable. Figure 9a presents a comparison of simulated SWE from four different sub-watersheds with the measurements from the Marquette weather station. The simulated SWE from different sub-watersheds follows closely with the measurements at the Marquette station. The timing of the snow melt is considered a crucial process for hydrological models in order to capture the appearance of flood peak for forecasting. The timing of the snow melt in different sub-watersheds shows a good agreement with observed spring snow melt in Figure 9a. Figure 9b plots the relationship of observed snow depth and temperature, which shows that the snow accumulation and melt closely follow the observed temperature variation.

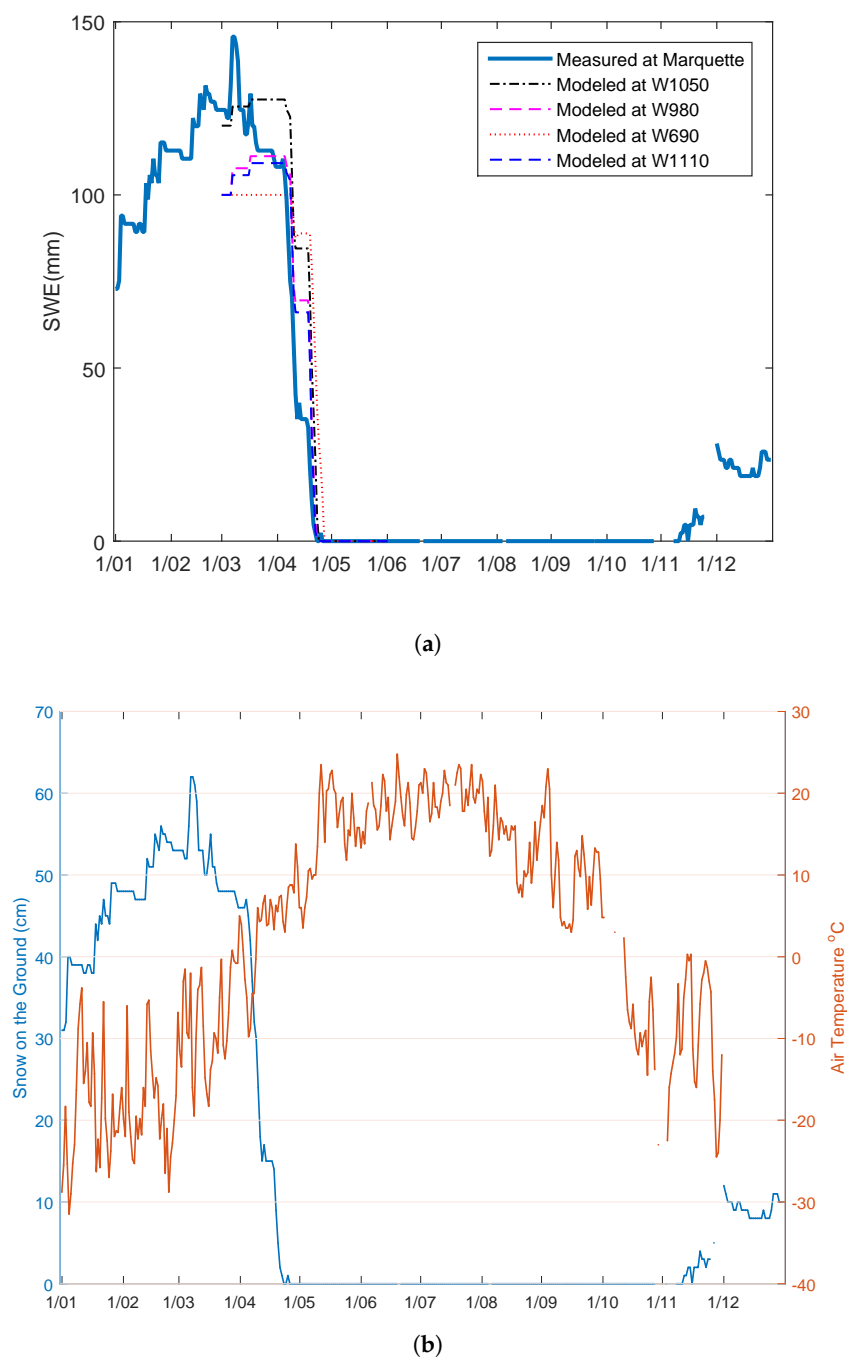


Figure 9. Validation of snow water equivalent (SWE) and timing of spring melt with temperature. (a) Comparison of measured and simulated snow water equivalent (SWE); (b) observed snow accumulation and melt pattern with temperature.

4.3. Snowmelt Model

4.3.1. Sensitivity of SMA Parameters

In the non-winter months, Prairie watersheds follow a sequence of wetting and drying periods. For a specific rainfall event, the initial moisture condition at the beginning of the rainfall event will have a major influence on a watershed's hydrological response. The initial soil moisture sensitivity on event modelling from this study revealed this fact as discussed in Section 4.3.2. Due to wetting and

drying during a continuous simulation, the model state reaches a value that is no longer dependent on the models' initial soil moisture saturation. In this study, the influence of initial soil moisture in a continuous HEC-HMS simulation is examined and found not sensitive (not presented).

Other important SMA parameters such as soil storage, soil percolation, tension storage, maximum infiltration and maximum canopy storage were tested within $\pm 40\%$ variation. The sensitivity of each parameter was tested against the simulated runoff volume at the outlet of the watershed. The percent change of parameters was done individually by $\pm 10\%$ increments while keeping other parameters unchanged. Results from each parameter sensitivity test to the percent change in runoff volume are presented in Table 4. The slope of each parameter's sensitivity was estimated using Theil-Sen's [41,42] non-parametric slope estimator. This method chooses the median slope among all lines through pairs of two-dimensional sample points. Ranking of each SMA parameter is performed using Theil-Sen's slope. It is evident from the Table 4 that the soil storage is ranked the most sensitive parameter for simulated stream flow in this watershed.

Table 4. Sensitivity of SMA parameters tested in Sub-watersheds W1100 and W870.

Percent Deviation (%)	Soil Storage (mm)	Soil Percolation (mm)	Tension Storage (mm)	Maximum Infiltration (mm/h)	GW1 Storage (mm)	Max Canopy Storage (mm)
<i>Sub-Watershed W1100</i>						
40	-20.06	-16.07	17.02	-15.20	-0.28	-9.73
30	-15.83	-12.98	11.40	-12.11	-0.24	-9.02
20	-11.04	-9.14	6.93	-8.46	-0.16	-7.36
10	-5.74	-4.87	3.36	-4.71	-0.08	-4.63
0	0.00	0.00	0.00	0.00	0.00	0.00
-10	6.73	5.54	-2.89	5.32	0.12	5.70
-20	15.43	11.79	-6.02	11.74	0.28	12.74
-30	27.78	18.60	-8.94	18.84	0.44	20.74
-40	48.12	26.39	-11.83	28.08	0.67	28.41
Slope ^a (b)	0.68	0.52	-0.33	0.51	0.01	0.50
Ranking	1	2	5	3	6	4
<i>Sub-Watershed W870</i>						
40	-16.67	-11.34	5.92	-8.19	-0.07	-6.41
30	-12.87	-8.80	4.53	-6.84	-0.07	-2.82
20	-8.86	-5.89	3.38	-4.65	-0.04	-1.37
10	-4.62	-3.23	1.42	-2.56	-0.03	-0.49
0	0.00	0.00	0.00	0.00	0.00	0.00
-10	5.19	3.12	-0.72	3.13	0.00	0.52
-20	10.81	6.36	-1.13	8.39	0.04	4.56
-30	17.53	10.45	-1.77	14.03	0.07	9.65
-40	25.09	13.38	-2.12	21.97	0.11	12.12
Slope (b)	0.50	0.31	-0.12	0.32	0.00	0.21
Ranking	1	3	5	2	6	4

^a Slope is estimated using Theil-Sen's method.

As shown in Table 4, other SMA parameters, such as maximum infiltration, soil percolation, maximum canopy storage and tension storage, can be ranked as sensitive. The SMA parameter sensitivity between Sub-watersheds W1100 and W870 also varies (i.e., soil percolation and maximum infiltration). A recent study presented by Roy et al. [43] demonstrated the variation of parameter sensitivity over different sub-watersheds. The sensitivity analysis of SMA parameters helps to understand the soil moisture accountability of the model.

4.3.2. Initial Soil Moisture

The event modelling of HEC-HMS was set up with the SMA loss method (Table 1) where the initial soil moisture condition was specified as the percentage of soil that is saturated with water at the beginning of simulation. The initial sub-watershed soil moisture (m^3m^{-3}) shown in Figure 4 is converted to soil saturation (%) using Equation (1) and used as the initial value for the HEC-HMS simulation.

In order to test the sensitivity of the initial soil moisture, the calibrated event model was used. Table 5 shows the sensitivity test of initial soil moisture over three sub-watersheds in the Sturgeon Creek. During calibration, the initial soil moisture of the W610 sub-watershed was set to 45.5% saturation, which is equivalent to $0.229 \text{ m}^3\text{m}^{-3}$ volumetric moisture. For the purpose of the sensitivity test, the input soil moisture is set to 60% soil saturation ($0.326 \text{ m}^3\text{m}^{-3}$) and 25% saturation ($0.125 \text{ m}^3\text{m}^{-3}$).

Table 5. Sensitivity of peak flow (m^3/s) and cumulative flow (1000 m^3) at different initial soil moistures. Results from three sub-watersheds (W610, W690, and W1000) are shown.

Initial Soil Moisture	Sub-Watershed Sensitivity				Watershed Sensitivity			
	Peak Flow (m^3/s)	Diff. ^a Peak (%)	Cum. Outflow (1000 m^3)	Cum. Flow Diff. (%)	Peak Flow (m^3/s)	Diff. Peak (%)	Cum. Outflow (1000 m^3)	Cum. Flow Diff. (%)
Sub-watershed W610, bulk density 1.32 gm/cm^3								
Calibration; $0.229 \text{ m}^3\text{m}^{-3}$ /45.5%.	0.229	0.4	42.9		3.9		1097	
$0.326 \text{ m}^3\text{m}^{-3}$ /60%	0.8	+100	94.6	+121	4.3	+10	1148	+5
$0.125 \text{ m}^3\text{m}^{-3}$ /25%	0.1	-75	12.3	-71	3.7	-5	1067	-3
Sub-watershed W960, bulk density 1.39 gm/cm^3								
Calibration; $0.291 \text{ m}^3\text{m}^{-3}$ /61.1%.	0.291	0.8	101.1		3.9		1097	
$0.215 \text{ m}^3\text{m}^{-3}$ /45%	0.4	-50	51.5	-49	3.8	-3	1048	-4
$0.125 \text{ m}^3\text{m}^{-3}$ /25%	0.2	-75	22.9	-77	3.8	-3	1020	-7
Sub-watershed W1000, bulk density 1.04 gm/cm^3								
Calibration; $0.243 \text{ m}^3\text{m}^{-3}$ /40%.	0.243	1.1	155.3		3.9		1097	
$0.364 \text{ m}^3\text{m}^{-3}$ /60%	1.9	+73	313.8	+102	4.2	+8	1254	+14
$0.151 \text{ m}^3\text{m}^{-3}$ /25%	0.5	-55	67.5	-57	3.8	-3	1010	-8

^a. Differences are calculated based on calibration output. A (+) sign indicates percent increase and a (-) sign indicates percent decrease from the calibration results.

The result of the initial soil moisture change to 60% shows an increase in peak and cumulative flow by 100% and 121%, respectively, for the sub-watershed. Increasing the initial soil moisture to 60% also resulted in an overall increase in the peak discharge and cumulative flow by 10% and 5%, respectively. The result of initial soil moisture change to 25% shows a decrease in peak and cumulative flow by 75% and 71%, respectively, for the sub-watershed. Decreasing initial soil moisture to 25% also resulted in an overall decrease in the peak discharge and cumulative flow by 5% and 3%, respectively.

Similar sensitivity tests on the initial soil moisture setting on two other sub-watersheds (i.e., W960 and W1000) were also performed. These are presented in Table 5, where high sensitivity on individual sub-watersheds can be seen as peak flow changes are in a range of 50%–75%, and cumulative flow changes are in a range of 49%–102% due to the change of initial soil moisture saturation on a sub-watershed. The overall impact on peak and cumulative flow due to the change of initial soil moisture on sub-watersheds is within a range of peak difference of 3%–8% and cumulative flow difference of 4%–14%. It can be concluded from these tests that the modelled peak flow and

cumulative output flow are very sensitive to the antecedent soil moisture condition. This confirms a similar study by [44,45], which concluded that HEC-HMS simulations are highly influenced by initial soil moisture on flood generation.

5. Conclusions

This study investigated the applicability of the Hydrologic Modelling System developed by the Hydrologic Engineering Center (HEC-HMS) in the Sturgeon Creek watershed; a snow melt-dominated watershed in Manitoba, Canada. Soil moisture was estimated from RADARSAT-2 satellite data and subsequently used to set the initial soil water content of the HEC-HMS model's event simulation. Event and continuous modelling of HEC-HMS has been performed in order to confirm the applicability of the model in Manitoba basins. Model performance measurements indicate that simulated flows are in good agreement with the observed results. The study also demonstrated that HEC-HMS and the temperature index method were able to accurately simulate the timing and magnitude of a spring snowmelt. Therefore, the model is well suited to determine runoff values for flood forecasting and other purposes.

Analysis of SMA parameters was performed to understand the sensitivity of each parameter on the movement and storage of water through different layers. Results from the analysis identified soil storage as the most sensitive parameter. A sensitivity analysis of initial soil moisture was performed to provide changes in peak flow and cumulative flow of the watershed and sub-watersheds under different saturations. The results confirm that peak flow in a snowmelt event is highly influenced by the initial soil moisture setting of the model.

Soil moisture information from RADARSAT-2 and the Fall Soil Moisture Survey of Manitoba were used to set the initial soil moisture states for two event simulations. Modelled flow data using the Fall Soil Moisture Survey did not agree well with observed flows. However, soil moisture data from RADARSAT-2 substantially improved the agreement between modelled and observed flows. These results demonstrate the ability of RADARSAT-2 to improve the performance of hydrology models over the Fall Soil Moisture Survey, which is based on field-collected data to define the soil moisture state. Satellites have a much greater ability to provide accurate soil moisture information with improved spatial/temporal resolution and coverage over the entire watershed.

This study supports the Hydrologic Forecast Center (HFC) and their efforts to find and to select an appropriate hydrology model for flood forecasting in Manitoba as recommended by the Flood Review Task Force [2]. The HFC has implemented MANAPI, which uses precipitation data from a sparse station network to define an antecedent precipitation index (API) map. MANAPI computes a single runoff value for a selected watershed from an event based on historical data. MANAPI is not capable of addressing complex watershed processes. Historical data for a graphical relationship of runoff-precipitation-API were not available for the Sturgeon Creek Watershed. Therefore, an MANAPI runoff value could not be compared with the event simulation.

This is the first attempt to use RADARSAT-2-derived soil moisture in hydrological modelling in an area where flooding events are caused by snowmelt. Despite the efforts to make the research comprehensive, further studies using RADARSAT-2-derived soil moisture for other Manitoba watersheds and for other years should be done to validate and enhance the findings of this study. Although this study only used one year (2014) of satellite soil moisture data for event modelling, the results indicate that the initial setting of RADARSAT-2-derived soil moisture can improve the performance of HEC-HMS and can be an appropriate tool for flood forecasting at the HFC in Manitoba.

Acknowledgments: This project was supported by the Science and Technology Branch (STB) of Agriculture and Agri-Food Canada and partially funded by the Government Related Initiatives Program (GRIP) of the Canadian Space Agency. We thank our colleagues from the Hydrologic Forecast Center (HFC) of Manitoba, who provided feedback that greatly assisted the research.

Author Contributions: H. McNairn, J. Powers, A. Merzouki and A. Bhuiyan conceived of and designed the experiments. A. Bhuiyan performed the experiments. A. Bhuiyan and J. Powers analysed the data. A. Merzouki contributed tools/processing RADARSAT-2 data. A. Bhuiyan wrote the paper.

Conflicts of Interest: The authors declare no conflict of interest.

Abbreviations

The following abbreviations are used in this manuscript:

AAFC	Agriculture and Agri-Food Canada
ECC	Environment and Climate Change Canada
MA	Manitoba Agriculture
SAR	Synthetic aperture radar
RADARSAT	Canadian remote sensing Earth observation satellite
HEC-HMS	Hydrologic Modelling System developed by the Hydrologic Engineering Center
SMA	Soil moisture accounting
MANAPI	Manitoba Antecedent Precipitation Index model
WSC	Water Survey Canada
HFC	Hydrologic Forecast Center
DEM	Digital elevation model
LiDAR	Light detection and ranging
IEM	Integral equation model
HH	Backscatter horizontal transmission and horizontal receive
VV	Backscatter vertical transmission and vertical receive
SCS	Soil Conservation Service
SWE	Snow water equivalent

References

1. Blais, E.L.; Clark, S.; Dow, K.; Rannie, B.; Stadnyk, T.; Wazney, L. Background to flood control measures in the Red and Assiniboine River Basins. *Can. Water Resour. J.* **2015**, doi:10.1080/07011784.2015.1036123.
2. Flood Review Task Force. Manitoba 2011 Flood Review Task Force Report. Report to the Minister of Manitoba Infrastructure and Transportation, 2013. Available online: https://www.gov.mb.ca/asset-library/en/2011flood/flood_review_task_force_report.pdf (accessed on 7 April 2016).
3. Rannie, W. The 1997 flood event in the Red River basin: Causes, assessment and damages. *Can. Water Resour. J.* **2015**, doi:10.1080/07011784.2015.1004198.
4. Stadnyk, T.; Dow, K.; Wazney, L.; Blais, E.L. The 2011 flood event in the Red River Basin: Causes, assessment and damages. *Can. Water Resour. J.* **2015**, 65–73.
5. Bower, S.S. Natural and unnatural complexities: Flood control along Manitoba's Assiniboine River. *J. Hist. Geogr.* **2010**, 36, 57–67.
6. Rasmussen, P.F. Evaluation of Flood Forecasting and Warning SSystem in Canada. 22nd Canadian Hyrotechnical Conference, 2015. Available online: http://www.nsercfloodnet.ca/files/Track_5_-_Presentation_-_Flood_forecasting_in_Canada_CSCE_2015.pdf (accessed on 7 April 2016).
7. Steenbergen, N.V.; Willems, P. Rainfall uncertainty in flood forecasting: Belgian case study of rivierbeek. *J. Hydrol. Eng.* **2014**, 19, doi:10.1061/(ASCE)HE.1943-5584.0001004.
8. Dietrich, J.; Schumann, A.H.; Redetzky, M.; Walther, J.; Denhard, M.; Wang, Y.; Pfutzner, B.; Büttner, U. Assessing uncertainties in flood forecasts for decision making: prototype of an operational flood management system integrating ensemble predictions. *Nat. Hazards Earth Syst. Sci.* **2009**, 9, 1529–1540.
9. Brocca, L.; Melone, F.; Moramarco, T.; Wagner, W.; Naeimi, V.; Bartalis, Z.; Hasenauer, S. Improving runoff prediction through the assimilation of the ASCAT soil moisture product. *Hydrol. Earth Syst. Sci.* **2010**, 14, 1881–1893.
10. Sutanudjaja, E.H.; van Beek, L.P.H.; de Jong, S.M.; van Geer, F.C.; Bierkens, M.F.P. Calibrating a large-extent high-resolution coupled groundwater-land surface model using soil moisture and discharge data. *Water Resour. Res.* **2014**, 50, 687–705.

11. Tramblay, Y.; Bouaicha, R.; Brocca, L.; Dorigo, W.; Bouvier, C.; Camici, S.; Servat, E. Estimation of antecedent wetness conditions for flood modelling in northern Morocco. *Hydrol. Earth Syst. Sci.* **2012**, *16*, 4375–4386.
12. Li, Y.; Grimaldi, S.; Walker, J.P.; Pauwels, V.R.N. Application of Remote Sensing Data to Constrain Operational Rainfall-Driven Flood Forecasting: A Review. *Remote Sens.* **2016**, *8*, doi:10.3390/rs8060456.
13. Massari, C.; Brocca, L.; Barbetta, S.; Papathanasiou, C.; Mimikou, M.; Moramarco, T. Using globally available soil moisture indicators for flood modelling in Mediterranean catchments. *Hydrol. Earth Syst. Sci.* **2014**, *18*, 839–853.
14. Xu, X.; Li, J.; Tolson, B.A. Progress in integrating remote sensing data and hydrologic modeling. *Appl. Meteorol. Climatol.* **2014**, *87*, 61–77.
15. McNairn, H.; Merzouki, A.; Pacheco, A. Estimating surface soil moisture using RADARSAT-2. In *International Archives of the Photogrammetry, Remote Sensing and Spatial Information Science*; Copernicus GmbH: Göttingen, Germany, 2010; pp. 576–579.
16. AAFC Information Bulletin 99-4. *Soils and Terrain. An Introduction to the Land Resource*. Rural Municipality of Rosser. *Information Bulletin 99-4*; Technical Report; Land Resources Unit, Brandon Research Centre, Research Branch, Agriculture and Agri-Food Canada: Winnipeg, MB, Canada, 1999.
17. AECOM Canada. *Sturgeon Creek Hydrodynamic Model and Economic Study, Project No.: F685 003 00 (4.6.1)*; Technical Report; Water Stewardship, Government of Canada: Winnipeg, MB, Canada, 2009.
18. Jacob, D.; Lorenz, P. Future trends and variability of the hydrological cycle in different IPCC SRES emission scenarios—A case study for the Baltic Sea Region. *Boreal Environ. Res.* **2009**, *14*, 100–113.
19. Thornthwaite, C.W. An Approach toward a Rational Classification of Climate. *Geogr. Rev.* **1948**, *38*, 55–94.
20. Feldman, A.D. *Hydrologic Modeling System HEC-HMS, Technical Reference Manual*; U.S. Army Corps of Engineers, Hydrologic Engineering Center HEC: Davis, CA, USA, 2000.
21. Alvarez, J.; Verhoest, N.E.C.; Casali, J.; Gonzalez-Audicana, M.; Lopez, J.J. RADARSAT based surface soil moisture retrieval on agricultural catchments of Navarre (Spain). In Proceedings of the 2004 IEEE International Geoscience and Remote Sensing Symposium, Anchorage, AK, USA, 20–24 September 2004; Volume 5, pp. 3507–3510.
22. Merzouki, A.; McNairn, H. A Hybrid (Multi-Angle and Multipolarization) Approach to Soil Moisture Retrieval Using the Integral Equation Model: Preparing for the RADARSAT Constellation Mission. *Can. J. Remote Sens.* **2015**, *41*, 349–362.
23. Eilers, P. *Sturgeon Creek Soil Moisture Monitoring Stations (SMMS); Soil and Landscape Classification*; Contract Number 3000528851. Technical Report; Science and Technology Branch, Agriculture and Agri-Food Canada: Winnipeg, Manitoba, 2013.
24. Schaffenberg, W.A. *Hydrologic Modeling System HEC-HMS, User Manual: Version 4.0*. U.S. Army Corps of Engineers, Hydrologic Engineering Center HEC, 609 Second Street, Davis, CA, USA, 2013.
25. U.S. Army Corps of Engineers. *Hydrologic Modeling System (HEC-HMS) Application Guide: Version 4.0*; Institute for Water Resources, Hydrologic Engineering Center: Davis, CA, USA, 2015.
26. Knebl, M.; Yang, Z.L.; Hutchison, K.; Maidment, D. Regional scale flood modeling using NEXRAD rainfall, GIS, and HEC-HMS/RAS: A case study for the San Antonio River Basin Summer 2002 storm event. *J. Environ. Manag.* **2005**, *75*, 325–336.
27. Du, J.; Qian, L.; Rui, H.; Zuo, T.; Zheng, D.; Xu, Y.; Xu, C.Y. Assessing the effects of urbanization on annual runoff and flood events using an integrated hydrological modeling system for Qinhuai River basin, China. *J. Hydrol.* **2012**, *464–465*, 127–139.
28. Haberlandt, U.; Radtke, I. Hydrological model calibration for derived flood frequency analysis using stochastic rainfall and probability distributions of peak flows. *Hydrol. Earth Syst. Sci.* **2014**, *18*, 353–365.
29. Fleming, M.; Neary, V. Continuous hydrologic modeling study with the hydrologic modeling system. *ASCE J. Hydraul. Eng.* **2004**, *9*, 175–183.
30. Gebre, S.L. Application of the HEC-HMS model for runoff simulation of upper blue Nile River Basin. *Hydrol. Curr. Res.* **2015**, *6*, 1–8.
31. Singh, W.R.; Jain, M.K. Continuous Hydrological Modeling using Soil Moisture Accounting Algorithm in Vamsadhara River Basin, India. *J. Water Res. Hydraul. Eng.* **2015**, *4*, 398–408.
32. Gyawali, R.; Watkins, D.W. Continuous Hydrologic Modeling of Snow-Affected Watersheds in the Great Lakes Basin Using HEC-HMS. *ASCE J. Hydraul. Eng.* **2013**, *18*, 29–39.
33. Hall, M.J. How well does your model fit the data? *J. Hydroinf.* **2001**, *3*, 49–55.

34. Krause, P.; Boyle, D.P.; Base, F. Comparison of different efficiency criteria for hydrological model assessment. *Adv. Geosci.* **2005**, *5*, 89–97.
35. Bardsley, W.E. A goodness of fit measure related to r^2 for model performance assessment. *Hydrol. Process.* **2013**, *27*, 2851–2856.
36. Nash, J.E.; Sutcliffe, J.V. River flow forecasting through conceptual models part I—A discussion of principles. *J. Hydrol.* **1970**, *10*, 282–290.
37. Henriksen, H.J.; Troldborg, L.; Nyegaard, P.; Sonnenborg, T.O.; Refsgaard, J.C.; Madsen, B. Methodology for construction, calibration and validation of a national hydrological model for Denmark. *J. Hydrol.* **2003**, *280*, 52–71.
38. Legates, D.R.; McCabe, G.J. Evaluating the use of goodness-of-fit measures in hydrologic and hydroclimatic model validation. *Water Resour. Res.* **1999**, *35*, 233–241.
39. Moriasi, D.N.; Arnold, J.G.; Liew, M.W.V.; Bingner, R.L.; Harmel, R.D.; Veith, T.L. Model evaluation guidelines for systematic quantification of accuracy in watershed simulations. *Am. Soc. Agric. Biol. Eng.* **2007**, *50*, 885–900.
40. Sturm, M.; Taras, B.; Liston, G.E.; Derksen, C.; Jonas, T.; Lea, J. Estimating snow water equivalent using snow depth data and climate classes. *J. Hydrometeorol.* **2010**, *11*, 1380–1394.
41. Theil, H. A rank-invariant method of linear and polynomial regression analysis, I, II, III. In Proceedings of the Royal Netherlands Academy of Sciences, Amsterdam, the Netherlands, 30 September 1950; pp. 1397–1412.
42. Sen, P.K. Estimates of the regression coefficient based on Kendall's tau. *J. Am. Stat. Assoc.* **1968**, *63*, 1379–1389.
43. Roy, D.; Begam, S.; Ghosh, S.; Jana, S. Calibration and validation of HEC-HMS model for a river basin in Eastern India. *J. Eng. Appl. Sci.* **2013**, *8*, 40–56.
44. Czigany, S.; Pirkhoffer, E.; Geresdi, I. Impact of extreme rainfall and soil moisture on flash flood generation. *J. Hung. Meteorol. Serv.* **2010**, *114*, 79–100.
45. Hegedus, P.; Czigany, S.; Balatonyi, L.; Pirkhoffer, E. Analysis of soil boundary conditions of flash Floods in a small basin in SW Hungary. *Cent. Eur. J. Geosci.* **2013**, *5*, 97–111.



© 2017 by the authors; licensee MDPI, Basel, Switzerland. This article is an open access article distributed under the terms and conditions of the Creative Commons Attribution (CC BY) license (<http://creativecommons.org/licenses/by/4.0/>).